

Dalton Transactions

Accepted Manuscript



This is an *Accepted Manuscript*, which has been through the Royal Society of Chemistry peer review process and has been accepted for publication.

Accepted Manuscripts are published online shortly after acceptance, before technical editing, formatting and proof reading. Using this free service, authors can make their results available to the community, in citable form, before we publish the edited article. We will replace this *Accepted Manuscript* with the edited and formatted *Advance Article* as soon as it is available.

You can find more information about *Accepted Manuscripts* in the [Information for Authors](#).

Please note that technical editing may introduce minor changes to the text and/or graphics, which may alter content. The journal's standard [Terms & Conditions](#) and the [Ethical guidelines](#) still apply. In no event shall the Royal Society of Chemistry be held responsible for any errors or omissions in this *Accepted Manuscript* or any consequences arising from the use of any information it contains.



Journal Name

ARTICLE

Synthesis of polymorph A-enriched Beta Zeolites in HF-Concentrated System

Guanqun Zhang^{a,d}, Bingchun Wang^a, Weiping Zhang^c, Mingrun Li^b and Zhijian Tian^{*,a,b}

Received 00th January 20xx,
Accepted 00th January 20xx

DOI: 10.1039/x0xx00000x

www.rsc.org/

ABSTRACT: Polymorph A-enriched Beta zeolites were synthesized by employing high HF concentrations in the synthesis medium. The polymorphic compositions of the synthesized Beta zeolites were determined by complementary characterizations of ¹⁹F NMR analysis and PXRD simulation. With a variety of SDAs, the high HF concentration (HF/SDA>1.0) in the synthesis medium results in the A-rich feature (55~65% A) of the Beta zeolites, while the moderate HF concentration only results in typical Beta. A systematic study on the synthesis conditions reveals the existence of a buffered system of H⁺ and F⁻ formed in the highly HF-concentrated medium. This buffer results in a small but continuous supply of F⁻ during zeolite crystallization, in contrast to the conventional fluoride route where all F⁻ are discharged all-at-once at the initial stage.

INTRODUCTION

Zeolites are crystalline materials defined by ordered microporous pores or cavities¹. For some zeolites like Beta², ITQ-39³, SSZ-26 and SSZ-33⁴, more than one forms of crystal structures (known as polymorphs) are able to exist and inter-grow in the zeolite. The different inter-growing extents of polymorphs would undoubtedly change the pore/cavity arrangement in zeolite structure and hence influence the stability and catalytic properties of zeolites⁵. Beta zeolite was among the first synthetic zeolites with three-dimensional large pores and high Si/Al ratios, and is widely applied in catalysis, separation and other fields⁶⁻⁹. Structural elucidation shows that Beta zeolite is an intergrowth of three closely related polymorphs, i.e. polymorph A, B and C^{2,10}. These polymorphs are built from epitaxial stacking of identical layer units. The different stacking ways of the neighboring layers build up these three polymorphs that possess similar twelve-ring pore sizes but different channel features: polymorph A has one chiral and two straight channels, polymorph B has one achiral sinusoidal and two straight channels, whereas polymorph C has three straight channels^{11,12}. The different channel structures of the three polymorphs endow them with different properties. The intrinsic chiral channel systems of polymorph A may be useful in chiral sorption and catalysis. For

instance, using the polymorph A-enriched Beta zeolite as the catalyst, Tong has reported a higher product enantioselectivity than by the typical Beta zeolite¹³. The three-dimensional straight channels of polymorph C would remarkably enhance the diffusion of reactants. Preceding research by Tomlinson¹⁴ and Li¹⁵ showed that the structure of polymorph A and B are almost thermodynamically equivalent while the structure of C is slightly less stable, indicating that those polymorphs tends to grow together instead separately. For decades endeavors in synthesis of Beta zeolites enriched in specific polymorphs have never faded. Nevertheless, despite the diversity of synthesis conditions employed, usually the synthesized Beta zeolites contain about 45% A, 55% B and trace amount of C^{16,17} (which is referred as "typical Beta"). The generally constant polymorphic composition of Beta makes the enrichment of specific polymorph quite challenging task. In 2001 by introducing Ge atoms in the synthesis Corma's group obtained pure polymorph C¹⁸. Later this group synthesized a Beta zeolite of 85% polymorph B by using a suitable structure-directing agent (SDA) and by adjusting H₂O/Si ratio in the synthesis medium¹⁹. Very recently, Yan's group has made great achievements in synthesizing A-enrich Beta containing 65% polymorph A. They demonstrated that the ultra-concentrated synthesis condition^{13,20-23} (H₂O/Si ≤ 1.12) and the partial decomposition of the tetraethylammonium hydroxide (TEAOH) are crucial to the enrichment of polymorph A in Beta zeolites. In these works, the polymorphic composition was determined by either PXRD refinement or PXRD simulation method which are suitable when no more than two polymorphs are present in the zeolite²⁴.

In this work, we present the syntheses of Beta zeolite under different HF concentrations (defined as HF/SDA ratio) with either pyrrole derivatives or tetraethylammonium hydroxide (TEAOH) as the SDA. Compositions of the three polymorphs in obtained materials were determined by employing ¹⁹F solid-state NMR analysis and powder X-ray diffraction simulation as complementary characterizations. When synthesized under high HF concentration,

^a Dalian National Laboratory for Clean Energy, Dalian Institute of Chemical Physics, Chinese Academy of Sciences, Dalian 116023, China. E-mail: tianz@dicp.ac.cn

^b State Key Laboratory of Catalysis, Dalian Institute of Chemical Physics, Chinese Academy of Sciences, Dalian National Laboratory for Clean Energy, 457 Zhongshan Road, Dalian 116023, China

^c State Key Laboratory of Fine Chemicals, Dalian University of Technology, 2 Linggong Road, Dalian 116024, China

^d University of Chinese Academy of Sciences, Beijing 100049, China
† Electronic Supplementary Information (ESI) available: PXRD and SEM of iBut/iPro/iPen-Beta(1.5); DIFFaX simulation of Beta zeolites of different proportion of polymorph A, B and C; ²⁹Si, ¹⁹F solid-state MAS NMR spectra of synthesis gels and zeolites of iBut/iPro/iPen/TEA-Beta. ¹⁹F liquid-state NMR of post-synthesis filtrates of iBut/TEA-Beta.

the Beta zeolites, directed by either of the SDAs, exhibit remarkable enrichment of polymorph A. Investigation on the fluoride species in the precursor gel and post-synthesis filtrates reveals the presence of a buffered system of H^+ and F^- in the synthesis medium, which controls the release of F^- for crystallization process and is thought to be responsible for the polymorphic enrichment in Beta zeolite.

EXPERIMENTAL SECTION

Synthesis of SDAs

Four SDAs were used in the synthesis to evaluate their influence on the polymorphic composition of Beta zeolite. Among them three pyrrole-based SDAs, i.e., N-isobutyl-N-methylpyrrolidinium hydroxide, N-isopropyl-N-methylpyrrolidinium hydroxide and N-isopentyl-N-methylpyrrolidinium hydroxide (denoted as iButOH, iProOH and iPenOH, respectively) were synthesized in laboratory. The synthetic steps are detailed in Supporting info. TEAOH, a common SDA in the synthesis of Beta, was purchased as 25wt% solution from Aladin and used as received.

Synthesis of Zeolite.

The synthetic procedure of zeolite Beta is based on the previous fluoride synthesis route with slight modifications¹² (see Supporting info for details). The molar composition of the final mixture is 1SDA : 2SiO₂ : 10H₂O : nHF. A summary of synthesis conditions is listed in Table 1. The products are denoted as iBut-Beta(n), iPro-Beta(n), iPen-Beta(n) and TEA-Beta(n), respectively, where the n value represents the HF/SDA ratio.

Characterization.

Powder X-ray powder diffraction (PXRD) was performed on a PANalytical X'Pert Pro diffractometer equipped with a Pixel detector using Cu K α 1 radiation ($\lambda=1.5406\text{\AA}$) operated at 40 mA and 40 kV with a scanning speed of 5°/min. Scanning electron microscope (SEM) was carried out on a Hitachi S4800 field-emission scanning electron microscope operating at 20kV. ²⁹Si and ¹⁹F solid-state magic angle spinning nuclear magnetic resonance (MAS NMR) data was collected on an Agilent DD2-500 MHz spectrometer with spinning rate of 13 kHz and 15 kHz, respectively. Liquid ¹⁹F and ²⁹Si NMR data were collected on a Bruker Avance III 500 MHz NMR spectrometer (frequency 470 MHz). ²⁹Si and ¹⁹F chemical shifts were referred to tetramethylsilane (TMS) and CFCl₃, respectively. N₂ isotherm was measured with a Micromeritics ASAP 2420 apparatus at 77 K. High-resolution transmission electron microscopy (HRTEM) images was performed on a FEI Tecnai F30 microscope operated at 300kV with a point resolution of 0.20 nm.

Simulation of powder X-ray diffraction (PXRD) pattern.

Powder X-ray diffraction patterns of the inter-grown structure of Beta zeolite was simulated using Program DIFFaX_v1813²⁴⁻²⁶. The unit cell parameters and planar translations of the building layer of zeolite Beta was extracted from the database of international zeolite association (see <http://izasc.biw.kuleuven.be/fmi/xsl/IZA-SC/ref.xsl>) as the starting model. The simulation was based on the random stacking of layers in zeolite structure. The instrumental broadening was shaped by the Pseudo-Voigt peak shape function wherein the parameters were set as 0.89, -0.32, 0.08 and 0.6 for u, v, w and σ respectively.

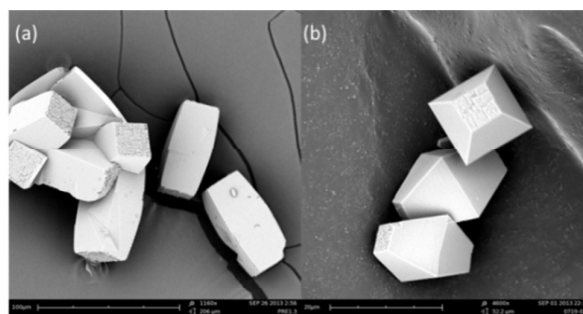


Figure 1. SEM images of (a) iBut-Beta(1.5) and (b) TEA-Beta(1.5).

RESULTS AND DISCUSSION

SEM images show that iBut-Beta(n), iPro-Beta(n) and iPen-Beta(n) zeolites have similar prism-like morphologies, whilst TEA-Beta(n) zeolites have truncated bipyramidal shapes (see Figure 1 and S1). As exhibited in Figure 1, the crystal of iBut-Beta(1.5) is constructed by four smoothly convex surfaces with two rough end planes, totally different from the flat planes of TEA-Beta(1.5). The curved shape of iBut-Beta zeolite is rarely seen in zeolite crystals which are usually featured by well-formed flat surfaces^{27,28} and is a sign of the unique faceting process of iBut-Beta.

PXRD patterns of iBut-Beta(n) and TEA-Beta(n) are shown in Figure 2. In the high-angle region ($2\theta > 10^\circ$), both iBut-Beta(n) and TEA-Beta(n) show characteristic diffraction peaks of "typical Beta" despite the increase of HF concentration in the synthesis. On the

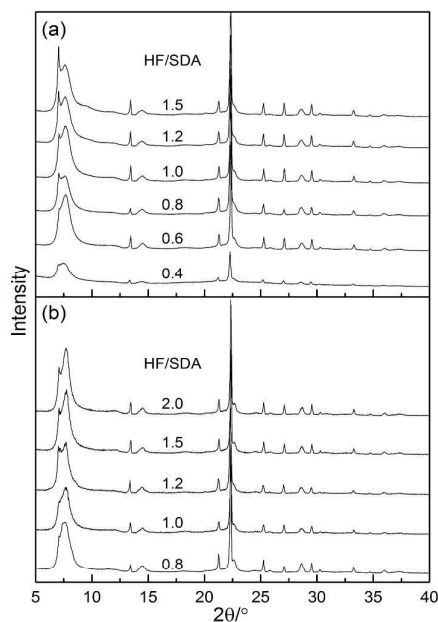


Figure 2. PXRD patterns of (a) iBut-Beta(n) and (b) TEA-Beta(n) samples synthesized with increasing HF/SDA ratios

other hand, in the low angle range ($2\theta < 10^\circ$), as HF concentration increases in the synthesis a significant peak change is present for both iBut-Beta(n) and TEA-Beta(n). More specifically, when the synthesis was performed at low HF concentration ($\text{HF}/\text{SDA} \leq 1/1$), the PXRD patterns of either iBut-Beta or TEA-Beta display only one broadened peak around 7.6° , which is in accordance with that of "typical Beta"; however, as HF concentration increases, the PXRD patterns exhibit a sharp peak at 7.03° with a shoulder at 7.68° for iBut-Beta(n) and a sharp peak at 7.08° with a shoulder at 7.68° for TEA-Beta(n). For iPro-Beta(n) and iPen-Beta(n) the peak features with increasing HF concentration is similar with that of iBut-Beta(n), as is shown in Figure S1.

^{29}Si solid-state MAS NMR spectra of iBut/iPro/iPen/TEA-Beta(1.5) displays no resonances below -105 ppm (see Figure S2), indicating the absence of Q^3 Si species²⁹. This spectral feature, together with the presence of only well-formed crystals in SEM images of iBut/iPro/iPen/TEA-Beta(1.5), confirms that the unusual PXRD patterns of these Beta samples rise from the intrinsic zeolitic structures rather than from impurities or structural defects.

Teacy² and Newsam¹⁰ referred the presence of sharp and broadened diffraction peaks of Beta zeolite to the polymorphism of the zeolite framework. Herein, by using program DIFFaX_v1813, we simulated a series of PXRD patterns for Beta zeolites containing different proportions of polymorph A, B and C (see Figure S3). Having different polymorphic compositions, these PXRD patterns basically the same in the range of $2\theta > 10^\circ$ but are quite different in $5\text{--}10^\circ$ range. Analysis from simulated PXRD patterns further reveals that, if a Beta zeolite is rich in polymorph A, a sharp peak will be present near 7.08° (the position of the characteristic peak of polymorph A); if rich in B a sharp peak be near 7.41° , and if rich in C a sharp peak be near 6.99° . Thus the presence of sharp diffraction peaks for iPro/iBut/iPen/TEA-Beta implies the enrichment of polymorph A and/or C in these Beta zeolites.

Structural analysis of Beta zeolites

Structurally, polymorph A is constructed by alternating stacking of building layers in either right-handed or left-handed manner around a four-fold screw axis; polymorph B is constructed by recurrent alternation of building layers in right- and left-handed fashion, and polymorph C is constructed by stacking of neighboring building layers with no lateral translations¹¹. The different stacking manners of identical building layers generate $[4^35^4]$ cages in polymorph A and B and $[4^6]$ cage in polymorph C. When Beta crystallizes in fluoride medium, the $[4^35^4]$ and $[4^6]$ cages accommodate one F^- per cage. Based on the type of cage that occludes F^- , ^{19}F NMR spectra shows two resonances at $-56\text{--}59$ ppm and $-65\text{--}69$ ppm for F^- in $[4^35^4]$ and $-36\text{--}39$ ppm for F^- in $[4^6]$ ¹⁶. Therefore ^{19}F NMR spectroscopy is a useful tool to probe the existence of polymorph C in Beta zeolite. Additionally, Blasco³⁰ showed that the proportion of polymorph C calculated from PXRD analysis agrees well with the ratio of $[4^6]/([4^6]+[4^35^4])$ from ^{19}F NMR spectra. Accordingly, the proportion of polymorph C of iBut/TEA-Beta(n) samples was estimated and listed in Figure S5 and S6. The result shows that at higher concentration iBut-Beta has a significant higher content of polymorph C than TEA-Beta. Additionally, the proportions of polymorph C estimated from iPro-/iPen-Beta(n) samples also show the high concentration of polymorph C (not shown).

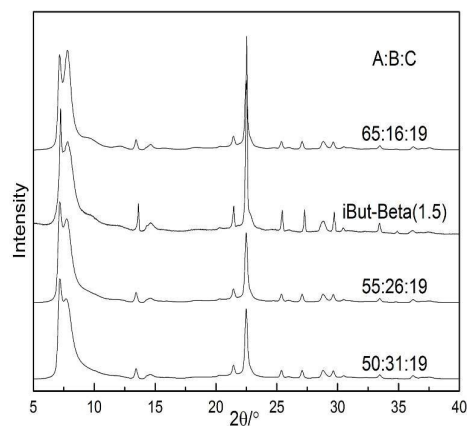


Figure 3. Comparison of the experimental pattern of iBut-Beta(1.5) and simulated PXRD patterns containing 19% polymorph C and different proportions of A and B.

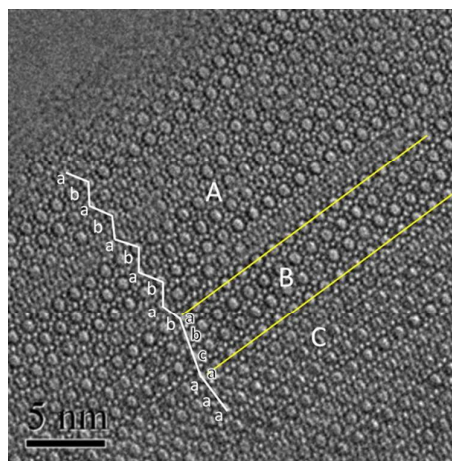


Figure 4. HRTEM image of iBut-Beta(1.5) taken along the $[100]$ direction. Note that every two polymorphs are separated by yellow lines along the polymorph boundaries.

After estimating the proportion of polymorph C, the proportions of polymorph A and B in iBut/TEA-Beta(n) samples were determined using PXRD simulation program DIFFaX (see Figure S8 and S9). We took the case of iBut-Beta(1.5) as an example. The sample contains 19% C as acquired via ^{19}F MAS NMR analysis. The PXRD pattern of iBut-Beta(1.5) was compared with a series of simulated PXRD patterns containing 19% C and different proportions of polymorph A and B (see Figure 3 and S7). As Figure 3 shows, the simulated pattern that contains 55~65% A, 20~30% B and 19% C fits best with iBut-Beta(1.5).

Figure 4 shows the HRETEM image of iBut-Beta(1.5) viewed along $[100]$ direction. The HRETEM image actually presents the projection of the zeolite framework in $[100]$ direction. In this projection, the chiral channel of polymorph A, the achiral zig-zag channel of polymorph B and the straight channel of polymorph C appears as the abab, abcabc, and aaaa arrangement of the twelve-ring pores,

respectively¹¹. The inter-grown domain contains all the three polymorphs as delineated by white lines. The boundaries of every two polymorphs contain large amounts of structural defects. From this domain ten layers of A, four layers of B and three layers of C is observed, which agrees to the polymorphic composition estimated from ¹⁹F NMR spectrum and PXRD simulation.

The estimated polymorphic compositions of all iBut-Beta(n) and TEA-Beta(n) samples are listed in table 1. It turns out that under low HF concentration ($0.4 \leq \text{HF}/\text{SDA} \leq 1$), all iBut-Beta(n) and TEA-Beta(n) zeolites contain similar polymorphic compositions with that of "typical Beta", and the choice of either TEOH or iButOH poses little influence on polymorphic composition of Beta zeolites. However, under high HF concentration the polymorphic composition of Beta zeolites is influenced both by the choice of SDA and by HF/SDA ratios. For iBut-Beta(n), when HF/SDA reaches 1.2 the proportion of A rises to 55~65% and stays unchanged despite further increase of HF concentration, while the proportion of C continuously ascends from 7% to 19%. Similar polymorphic compositions are also estimated for iPro-Beta and iPro-Beta. For TEA-Beta(n), when HF/SDA reaches 1.5 the proportion of A rises to a constant value of 55~65% whereas the proportion of C is basically unchanged (~2%) within the HF/SDA range of 0.8~2.0. Therefore the polymorph A-enriched iBut-Beta is obtained from the synthesis with HF/SDA ratios larger than 1.0, and A-enriched TEA-Beta is obtained from the synthesis with HF/SDA ratios larger than 1.2. In Yan's report, the A-enriched Beta zeolite contains approximately 60~65% polymorph A¹³ that is similar with the proportion of A of iBut/iPro/iPen/TEA-Beta(n) synthesized in our work. However, the iBut/iPro/iPen-Beta(n) synthesized under high HF concentration also contain a large proportion of polymorph C.

Table 1. Polymorphic compositions of iBut-Beta(n) and TEA-Beta(n) samples

SDA	n	C% ^[a]	A% ^[b]	B% ^[b]
iButOH	0.4	6	40~50	45~55
iButOH	0.6	5	40~50	45~55
iButOH	0.8	8	45~55	35~45
iButOH	1.0	7	50~60	35~45
iButOH	1.2	12	55~65	30~40
iButOH	1.5	19	55~65	20~30
TEAOH	0.8	4	40~50	45~55
TEAOH	1.0	4	40~50	45~55
TEAOH	1.2	3	40~50	45~55
TEAOH	1.5	3	55~65	30~40
TEAOH	2.0	2	55~65	30~40

^a values derived from ¹⁹F MAS NMR spectra.

^b values estimated from DIFFaX simulation.

Fluoride species in zeolite synthesis.

In zeolite synthesis HF acts both as the mineralizer and as the pH adjustor, so the increase in HF concentration not only increases the amount of fluoride in the synthesis medium but also decreases the overall pH value. The change of pH value would further influence the state of fluoride species in the synthesis medium. In conventional fluoride-route Beta zeolite crystallizes in neutral medium produced by equivalent amount of HF and alkaline SDA in the synthesis medium¹². Tsuneji³¹ studied the state of fluoride species in the synthesis of Beta with equivalent amount of HF and TEOH and discovered that the vast majority of fluoride species in the precursor gel are F⁻ in the form of TEAF. Nevertheless, as stated by Cundy³² and Koller³³, as synthesis medium becomes acidic, F⁻ reacts with silicate in complicated ways forming various fluoride species such as Si(OH)_nF³⁻ⁿ and SiF_n⁴⁻ⁿ. Guth et al.³⁴ also concluded that SiF₆²⁻ becomes more prominent in the synthesis as fluoride concentration increases. Figure 5a shows ¹⁹F solid-state MAS NMR spectra of the precursor gels of iBut-Beta(n). Two resonances can be observed corresponding to the presence of two different fluoride species in precursor gels. The first species, having a ¹⁹F NMR resonance at -118 ppm, is ascribed to F⁻ in the form of iButF^{35, 36}, and denoted as free-F⁻ (and F⁻ entrapped in [4⁶] or [4³⁵4] cage is denoted as entrapped-F⁻). The second species has a ¹⁹F NMR resonance at -128 ppm; furthermore, the gel of iBut-Beta(1.5) which only presents the ¹⁹F NMR resonance -128 ppm was subject to ²⁹Si solid-state MAS NMR and shows a resonance at -188 ppm^{37, 38} corresponding to hexa-coordinated Si⁴⁺ in SiF₆^{2-36, 39} (see Figure 5b). So the second species in ¹⁹F NMR spectra is unambiguously assigned as SiF₆²⁻ in the form of iBut₂SiF₆. No other fluoride species, such as SiF₅²⁻ or Si(OH)₃F, are detected these precursor gels. As Figure 5a shows, when HF/SDA ratio in the synthesis is smaller than 0.6 (with the synthesized zeolites being typical Beta), only free-F⁻ is present in the gels; as HF/SDA ratio grows larger (with the synthesized zeolites being A-enrich Beta), SiF₆²⁻ appears and grows with F⁻ progressively disappearing. The case for the precursor gels of TEA-Beta(n) is similar: as HF/SDA grows SiF₆²⁻ becomes prominent over F⁻ and eventually exists as the only fluoride species (see Figure S10). In summary, the enrichment of polymorph A in

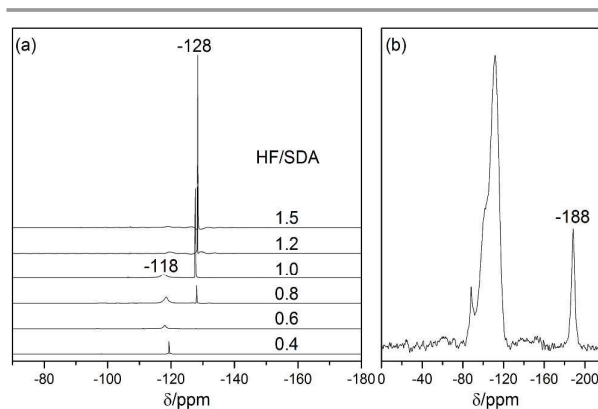


Figure 5. (a) ¹⁹F MAS NMR spectra of the precursor gels of iBut-Beta with increasing input of HF/SDA ratios (from bottom to top); (b) ²⁹Si MAS NMR spectrum of the precursor gel of iBut-Beta(1.5).

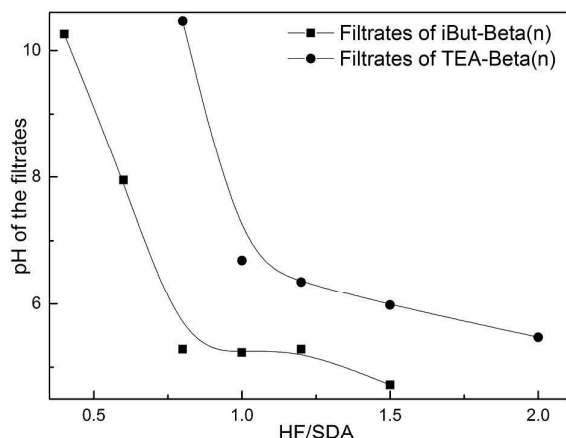
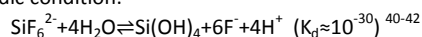


Figure 6. Correlation between the increasing input HF/SDA ratios and the pH values of post-synthesis filtrates of (a) iBut-Beta(n) and (b) TEA-Beta(n) samples.

Beta is coincided with the formation of SiF_6^{2-} in the precursor.

Figure 6 displays the correlation between the input HF/SDA ratio in the synthesis of iBut/TEA-Beta(n) and the pH values of the corresponding post-synthesis filtrates. As input HF/SDA increases, the pH value of the filtrates first descends drastically (within the pH range where all the crystallized products are typical Beta) but then descends in a much gentler way (within the pH range where all the crystallized products are A-enriched Beta), implying the existence of a pH buffer within the HF/SDA range of 1.0~1.5 for iBut-Beta(n) and 1.2~2.0 for TEA-Beta(n). In addition, the presence of this buffer parallels the predominance of SiF_6^{2-} in the filtrates, as evidenced by ^{19}F liquid-state NMR (Figure S11).

An equilibrium can explain the correlation between F^- and SiF_6^{2-} in slightly acidic condition:



This equilibrium indicates that a buffer of H^+ and F^- could be produced by the presence of SiF_6^{2-} . In a recent research, Corma's group discovered a buffer of F^- formed by K_2SiF_6 in the synthesis medium and proved that that buffer is key to formation of the pure polymorph C⁴³. We thought that the presence of such a F^- -buffer in our work is responsible for the polymorphic enrichment of Beta zeolites.

Evolution of fluoride species during crystallization

Fluoride species plays a crucial role in nucleation and crystal growing process of Beta zeolite. Studies by Cambor⁴⁴, Barrett⁴⁵ and Larlus⁴² et al., show that fluoride help mobilize silica species, stabilize small subunits like $[4^6]$ cages, pair with the OSDA cation and decrease the crystallization rate. Due to the large size, SiF_6^{2-} is not likely to enter and stabilize framework subunits like $[4^6]$ as F^- does. In fact, as we discovered, with high HF/SDA input the fluoride species in the precursor gel of Beta are exclusively SiF_6^{2-} , however the only fluoride species detected in the cleansed zeolite are F^- . Thus there should be a transport route of fluoride from SiF_6^{2-} to entrapped- F^- in zeolite structure. Barrett⁴⁶ and Zones⁴⁷ discussed the role of SiF_5^- and SiF_6^{2-} as dynamic species in the break-formation of Si-O-Si bonds during crystallization, and proposed that such

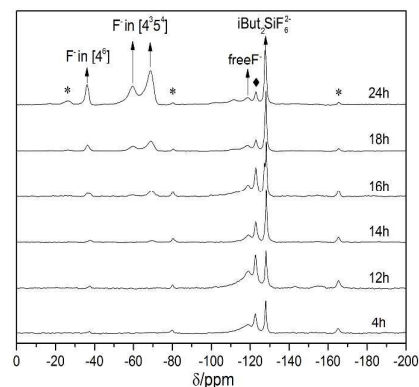


Figure 7. ^{19}F MAS NMR spectra of iBut-Beta(1.5) synthesized at different time. The asterisks are spinning side bands and the diamond the background signal arising from fluorine species in NMR detector.

species helps to transport highly fluorinated silicate species to solution, resulting in the slow-down of the nucleation rate of the zeolite. Similarly, the replacement of F^- by SiF_6^{2-} in the starting materials should lead to a different crystallization process of Beta zeolite from that of conventional fluoride-route synthesis. The unwashed products of iBut-Beta(1.5) were synthesized at different time and then dried at 353K and subject to ^{19}F solid-state MAS NMR (see Figure 7) to track the evolution of SiF_6^{2-} along zeolite crystallization.

As shown in Figure 5a, in the precursor gel of iBut-Beta(1.5) SiF_6^{2-} is the only fluoride species. However, since the initial stage of crystallization, a small part of free- F^- is also present in reaction materials. The presence of F^- in the materials is attributable to the condensation of the silanol groups during crystallization, which generated OH^- ^{46,48} to shift the equilibrium between F^- and SiF_6^{2-} in favor of F^- . At longer crystallizing time the F^- entrapped in $[4^6]$ and $[4^35^4]$ cages starts to emerge. It can be inferred from Figure 7 that during the whole crystallization process (note that iBut-Beta(1.5) is of high crystallinity in 24h) the vast majority of fluoride is stored in the form of SiF_6^{2-} rather than F^- , and the transfer of fluoride follows a " $\text{SiF}_6^{2-} \rightarrow \text{free-F}^- \rightarrow \text{entrapped-F}^-$ " route. Under high HF concentration the F^- -buffer maintains a relatively constant and low concentration of F^- in the synthesis medium. Thus a small but continuous amount of F^- is released in the synthesis medium, in contrast to the all-at-once discharge of F^- in conventional fluoride route. Owing to the insufficient supply of F^- the nucleation process of Beta zeolite should be relatively slow. Probably such a slow nucleation allows for a more ordered successive stacking of building layers and results in the enrichment of polymorph A, C in iBut/iPro/iPen-Beta and the enrichment of polymorph A in TEA-Beta.

CONCLUSIONS

In summary, we have presented a novel synthesis route to A-enriched Beta zeolites. The polymorphic composition of the synthesized materials was solved by using complementary characterizations of ^{19}F MAS NMR and PXRD simulation method. Investigation on the synthesis conditions reveals that when large amount of HF is present in the synthesis medium, a vast majority of F^- converts to SiF_6^{2-} and a buffered system of H^+ and F^- formed in the synthesis medium. This buffer restricts the release of F^- to a small but continuous supply for crystallization process, which may be the reason for the polymorphic enrichment in Beta zeolite.

Acknowledgements

This work is supported by the Strategic Guide Scientific Special fund of Chinese Academy of Sciences (XDA07020300).

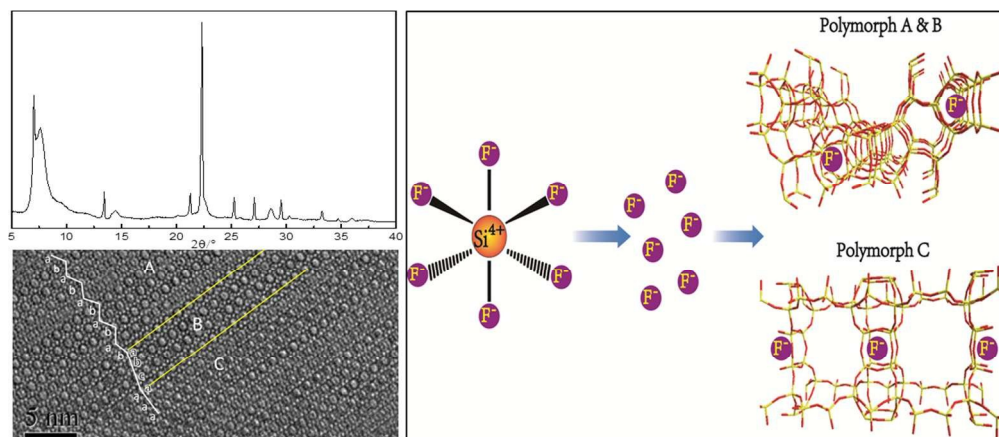
Notes and references

- M. E. Davis, *Nature (London, U. K.)*, 2002, **417**, 813-821.
- M. M. J. Treacy and J. M. Newsam, *Nature (London)*, 1988, **332**, 249-251.
- T. Willhammar, J. Sun, W. Wan, P. Oleynikov, D. Zhang, X. Zou, M. Moliner, J. Gonzalez, C. Martinez, F. Rey and A. Corma, *Nat. Chem.*, 2012, **4**, 188-194.
- R. F. Lobo, M. Pan, I. Chan, R. C. Medrud, S. I. Zones, P. A. Crozier and M. E. Davis, *The Journal of Physical Chemistry*, 1994, **98**, 12040-12052.
- T. Willhammar and X. Zou, *Z. Kristallogr. - Cryst. Mater.*, 2013, **228**, 11-27.
- T. De Baerdemaeker, B. Yilmaz, U. Müller, M. Feyen, F.-S. Xiao, W. Zhang, T. Tatsumi, H. Gies, X. Bao and D. De Vos, *Journal of Catalysis*, 2013, **308**, 73-81.
- Z. Chen, B. Holmberg, W. Li, X. Wang, W. Deng, R. Munoz and Yan, *Chemistry of Materials*, 2006, **18**, 5669-5675.
- C. Chen, Q. Wu, F. Chen, L. Zhang, S. Pan, C. Bian, X. Zheng, X. Meng and F.-S. Xiao, *Journal of Materials Chemistry A*, 2015, **3**, 5556-5562.
- A. Corma, L. T. Nemeth, M. Renz and S. Valencia, *Nature*, 2001, **412**, 423-425.
- J. M. Newsam, M. M. J. Treacy, W. T. Koetsier and G. C. B. De, *Proc. R. Soc. London, A*, 1988, **420**, 375-405.
- A. W. Burton, S. Elomari, I. Chan, A. Pradhan and C. Kibby, *The Journal of Physical Chemistry B*, 2005, **109**, 20266-20275.
- M. A. Cambor, A. Corma and S. Valencia, *Chem. Commun. (Cambridge)*, 1996, DOI: 10.1039/cc9960002365, 2365-2366.
- M. Tong, D. Zhang, W. Fan, J. Xu, L. Zhu, W. Guo, W. Yan, J. Yu, S. Qiu, J. Wang, F. Deng and R. Xu, *Sci. Rep.*, 2015, **5**, 11521.
- S. M. Tomlinson, R. A. Jackson and C. R. A. Catlow, *J. Chem. Soc., Chem. Commun.*, 1990, 813-816.
- Q. Li, A. Navrotsky, F. Rey and A. Corma, *Microporous and Mesoporous Materials*, 2003, **59**, 177-183.
- M. A. Cambor, P. A. Barrett, M.-J. Diaz-Cabanias, L. A. Villaescusa, M. Puche, T. Boix, E. Perez and H. Koller, *Microporous Mesoporous Mater.*, 2001, **48**, 11-22.
- S. I. Zones, A. W. Burton, G. S. Lee and M. M. Olmstead, *J. Am. Chem. Soc.*, 2007, **129**, 9066-9079.
- A. Corma, M. T. Navarro, F. Rey, J. Rius and S. Valencia, *Angew. Chem., Int. Ed.*, 2001, **40**, 2277-2280.
- A. Corma, M. Moliner, A. Cantin, M. J. Diaz-Cabanias, J. L. Jorda, D. Zhang, J. Sun, K. Jansson, S. Hovmoeller and X. Zou, *Chem. Mater.*, 2008, **20**, 3218-3223.
- J. Sun, G. Zhu, Y. Chen, J. Li, L. Wang, Y. Peng, H. Li and S. Qiu, *Microporous Mesoporous Mater.*, 2007, **102**, 242-248.
- Y. W. GUO Wen, XU Ruren, WANG Yongrui, MU Xuhong, *Chemical Journal of Chinese Universities*, 2014, **35**, 1363-1368.
- T. Lu, P. Gao, J. Xu, Y. Wang, W. Yan, J. Yu, F. Deng, X. Mu and R. Xu, *Chinese Journal of Catalysis*, 2015, **36**, 889-896.
- M. Tong, D. Zhang, L. Zhu, J. Xu, F. Deng, R. Xu and W. Yan, *CrystEngComm*, 2016, DOI: 10.1039/C6CE00043F.
- A. V. Radha, C. Shivakumara and P. V. Kamath, *Clays Clay Miner.*, 2005, **53**, 520-527.
- M. M. J. Treacy, M. W. Deem and M. J. Newsam, *DIFFaX v1.812*, 2005, available at <http://www.public.asu.edu/~mtreacy/DIFFaX.html>.
- M. Casas-Cabanias, J. Rodríguez-Carvajal, J. Canales-Vázquez, Y. Lalgaité, P. Lacorre and M. R. Palacín, *J. Power Sources*, 2007, **174**, 414-420.
- A. Petushkov, G. Merilis and S. C. Larsen, *Microporous Mesoporous Mater.*, 2011, **143**, 97-103.
- Q. H. Xia, S. C. Shen, J. Song, S. Kawi and K. Hidajat, *J. Catal.*, 2003, **219**, 74-84.
- T. Willhammar, A. W. Burton, Y. Yun, J. Sun, M. Afeworki, K. G. Strohmaier, H. Vroman and X. Zou, *J. Am. Chem. Soc.*, 2014.
- J. A. Vidal-Moya, T. Blasco, A. Corma, M. T. Navarro and F. Rey, *Stud. Surf. Sci. Catal.*, 2004, **154B**, 1289-1294.
- H. Jon, Y. Oumi, K. Itabashi and T. Sano, *J. Cryst. Growth*, 2007, **307**, 177-184.
- C. S. Cundy and P. A. Cox, *Microporous and Mesoporous Materials*, 2005, **82**, 1-78.
- H. Koller, A. Wölker, L. A. Villaescusa, M. J. Díaz-Cabañas, S. Valencia and M. A. Cambor, *J. Am. Chem. Soc.*, 1999, **121**, 3368-3376.
- J. L. Guth, H. Kessler, J. M. Higel, J. M. Lamblin, J. Patarin, A. Seive, J. M. Chezeau and R. Wey, in *Zeolite Synthesis*, American Chemical Society, 1989, vol. 398, ch. 13, pp. 176-195.
- L. Delmotte, M. Souillard, F. Guth, A. Seive, A. Lopez and J. L. Guth, *Zeolites*, 1990, **10**, 778-783.
- J. M. Miller, *Prog. Nucl. Magn. Reson. Spectrosc.*, 1996, **28**, 255-281.
- S. A. Axon and J. Klinowski, *J. Chem. Soc., Faraday Trans.*, 1993, **89**, 4245-4248.
- J. F. Stebbins, *Nature*, 1991, **351**, 638-639.
- P. Caultet, L. Delmotte, A. C. Faust and J. L. Guth, *Zeolites*, 1995, **15**, 139-147.
- E. T. Urbansky, *Chem. Rev.*, 2002, **102**, 2837-2854.
- W. F. Finney, E. Wilson, A. Callender, M. D. Morris and L. W. Beck, *Environmental Science & Technology*, 2006, **40**, 2572-2577.
- O. Larlus and V. Valtchev, *Microporous Mesoporous Mater.*, 2006, **93**, 55-61.
- Á. Cantin, A. Corma, M. J. Díaz-Cabañas, J. L. Jordá, M. Moliner and F. Rey, *Angew. Chem. Int. Ed.*, 2006, **45**, 8013-8015.
- M. A. Cambor, L. Villaescusa and M. Diaz-Cabanias, *Top. Catal.*, 1999, **9**, 59-76.

Journal Name

ARTICLE

45. P. A. Barrett, E. T. Boix, M. A. Cambor, A. Corma, M. J. Diaz-Cabanas, S. Valencia and L. A. Villaescusa, 1999.
46. P. A. Barrett, M. A. Cambor, A. Corma, R. H. Jones and L. A. Villaescusa, *The Journal of Physical Chemistry B*, 1998, **102**, 4147-4155.
47. S. I. Zones, R. J. Darton, R. Morris and S.-J. Hwang, *J. Phys. Chem. B*, 2005, **109**, 652-661.
48. R. K. Iler, *Soil Science*, 1955, **80**, 86.



210x90mm (150 x 150 DPI)